Dalton Transactions

RSC Publishing

PAPER

View Article Online
View Journal | View Issue

Cite this: *Dalton Trans.*, 2013, **42**, 4994

Synthesis, conjugation and relaxation studies of gadolinium(III)-4-benzothiazol-2-yl-phenylamine as a potential brain specific MR contrast agent

Nisha Saini,[a,b] Raunak Varshney,[a] Anjani K. Tiwari,*[a] Ankur Kaul,[a] Michele Allard,[c] M. P. S. Ishar[b] and Anil K. Mishra*[a]

Magnetic resonance (MR) imaging is widely used in clinical research to map the structural and functional organization of the brain. We have designed and synthesized a Gd-based specific MR contrast agent that binds to regions in the brain. The presented compound {4-[(4-benzothiazol-2-yl-phenylcarbamoyl)-methyl]-7,10-bis-carboxymethyl-1,4,7,10-tetraazacyclododec-1-yl} acetic acid (DO3A-BT) was synthesized by conjugating the chloroacetylated product of 4-benzothiazol-2-yl-phenylamine with a trisubstituted cyclen. The lanthanide complex (Ln–DO3A-BT) was evaluated *in vitro* for both MR (Gd–DO3A-BT) and optical (Eu–DO3A-BT) imaging applications. The complex Gd–DO3A-BT displays a relaxivity of r_1 = 4.18 mM^{-1} s^{-1} at 4.7 T which is 1.2 times greater than Dotarem and significantly higher than the brain specific MR contrast agent Luxol Fast Blue (LFB). The protonation constant of the ligand (pK_{a1} = 9.91, pK_{a2} = 8.22, pK_{a3} = 5.01) and the stability constant of the complex formed between Gd(III), Eu(III) and Ca(II) and ligand DO3A-BT (log β_{GdL} = 18.4, log β_{EuL} = 18.3, log β_{Zn2L} = 7.1, log β_{Ca2L} = 6.3) were recorded by potentiometric titration. The constants reflect the high stability of the ligand with lanthanides compared with endogenous metal ions. The transmetalation stability of Gd–DO3A-BT toward Zn proved to be excellent with a rate constant of 3.07 × 10^{-5} s^{-1} which is in line with other tetraazatetraacetic acid (DOTA)–monoamide complexes. The hydration number (q) was found to be 0.92, and is calculated from the difference in the luminescence lifetime of Eu–DO3A-BT in H_2O and D_2O solutions to determine the coordination state of this complex. The *in vivo* biodistribution of ^{99m}Tc–DO3A-BT in BALB/c mice showed a brain uptake of 1.2% ID g^{-1} at 2 min post injection when injected with mannitol which disrupts the blood–brain-barrier (BBB) due to osmotic shock. *In vitro* binding on the brain homogenate revealed a high uptake by the neuronal/glial cells for *in vivo* applications.

Received 1st June 2012,
Accepted 7th January 2013

DOI: 10.1039/c2dt32391e

www.rsc.org/dalton

Introduction

Magnetic resonance imaging (MRI) is emerging as a powerful tool for studying the microstructure of many tissues, including the architecture of the human brain. There is an important need for increased MR research for contrast agents with improved soft-tissue contrast which will enhance the capacity of MRI to provide functional information of different regions.[1,2] The longitudinal MRI studies can provide a non-invasive tool to understand brain functions, as well as measure the effects of drug and other therapeutic interventions with a high degree of specificity.

The advantage of using MRI for neuroscience is to perform imaging in conjunction with contrast agents. Polyaminopolycarboxylic acid complexes of lanthanides have widespread application as contrast agents in MRI imaging. Thus the coordination chemistry of lanthanide complexes of polyaminocarboxylates has become important in biomedical science for MR contrast agents[3–6] and as luminescent probes.[7,8] The MR images are achieved by changing the magnetic relaxation times of the protons in tissue-contained water. These images are enhanced by the use of contrast agents as they increase the longitudinal and transverse relaxation rate of the water protons which contribute to the contrast of the image.[9] Gadolinium(III) ions are an ideal choice due to their high spin state (s = 7/2), high magnetic moment, slow electronic relaxation rate and labile hydration sphere for water exchange.[10–16] According to the Soloman–Bloembergen–Morgan equation theory high relaxivity can be obtained in the presence of a greater number of inner sphere water molecules q; an optimally short water residence time τ_m; and a slow tumbling rate τ_r while

[a]*Division of Cyclotron and Radio-Pharmaceutical Sciences, Institute of Nuclear Medicine and Allied Sciences, Brig S. K. Majumdar Road, Delhi-54, India. E-mail: akmishra63@gmail.com, anjani7797@rediffmail.com; Tel: +91-11-2390511709968314130*
[b]*Department of Pharmaceutical Sciences, Guru Nanak Dev University, Amritsar-005, India*
[c]*Universite de Bordeaux, UMR-CNRS 5287-EPHE, Bordeaux, France*

maintaining sufficient thermodynamic stability.[17–19] The complexation with numerous ions such as Ca^{2+}, Zn^{2+}, Cu^{2+} and precipitation of Gd^{3+} salts may contribute to the *in vivo* dissociation of the Gd^{3+} complexes. Gd forms thermodynamically and kinetically stable complexes with polyaminopolycarboxylate-type ligands such as the tetraazatetraacetic acid macrocycle (DOTA) and diethylenetetraamine pentaacetic acid (DTPA).[20,21]

The action of MRI contrast agents requires one or more water molecules to be coordinated to the paramagnetic metal ion, and these are important in determining the molar relaxivity of the agent. Thus the structural dynamics of MR contrast agents are very important for clinical aspects and can be measured by the luminescence decay rate and the high resolution absorption spectra of the Eu^{3+} complex.[22–24] More precise determination of the complex hydration state (q) gives unique information on the local symmetry and specification of $^7F_0 \rightarrow {}^5D_0$ band.

The selected benzothiazole moiety is present in various dyes such as primuline and thioflavin which possess the potential to fluorescently stain diseased brain tissues.[25,26] Recently, an attempt has been made to use Luxol Fast Blue (LFB), a histological stain for brain tissue with a paramagnetic copper core, as a MR probe. LFB shows a low relaxivity (r_1 = 0.09 mM^{-1} s^{-1} at 4.7 T) and a modest solubility[27] but the longitudinal relaxivity of DO3A-BT is ~34 times more than that of LFB. On the other hand, biodistribution studies of the thioflavin analogue *i.e.* [^{125}I]IMPY[28] in normal mice exhibited a brain uptake of 2.2% ID g^{-1} with a fast washout. However, Gd–DO3A-BT has lower brain permeability than [^{125}I]IMPY and there is no exposure to ionizing radiation which makes our compound a more promising candidate. Hence the encouraging *in vitro* and *in vivo* studies of DO3A-BT supports the choice of this derivative for further evaluation in brain research. Thus with the aim to synthesize a bifunctional probe which can be applied in brain targeted magnetic resonance imaging (MRI) and optical imaging. To achieve this, we conjugated an arylbenzothiazole moiety with a macrocyclic ring. The compounds were characterized by NMR and ESI-MS spectroscopy and their relaxivity, luminescence lifetime and biological applications were evaluated.

Results and discussion

Design and synthesis of the contrast agent

4-Benzothiazol-2-yl-phenylamine **3** was synthesized from 2-amino-benzenethiol and 4-aminobenzoic acid using polyphosphoric acid. It was chloroacetylated to obtain *N*-(4-benzothiazol-2-yl-phenyl)-2-chloroacetamide **4**. The chloroacetylated product was conjugated to a trisubstituted cyclen to yield the desired compound *i.e.* 10-[*N*-(4-benzothiazol-2-yl-phenylcarbamoyl)-methyl]-1,4,7-tri(carbobutoxymethane)-1,4,7,10-tetraazacyclododecane **6**. Compound **6** was deprotected to remove the *tert*-butyl group using trifluoroacetic acid at 0 °C, and, on further complexation with $GdCl_3$ and $EuCl_3$, gave Gd–DO3A-BT **8** and Eu–DO3A-BT **9** respectively (Scheme 1). The above

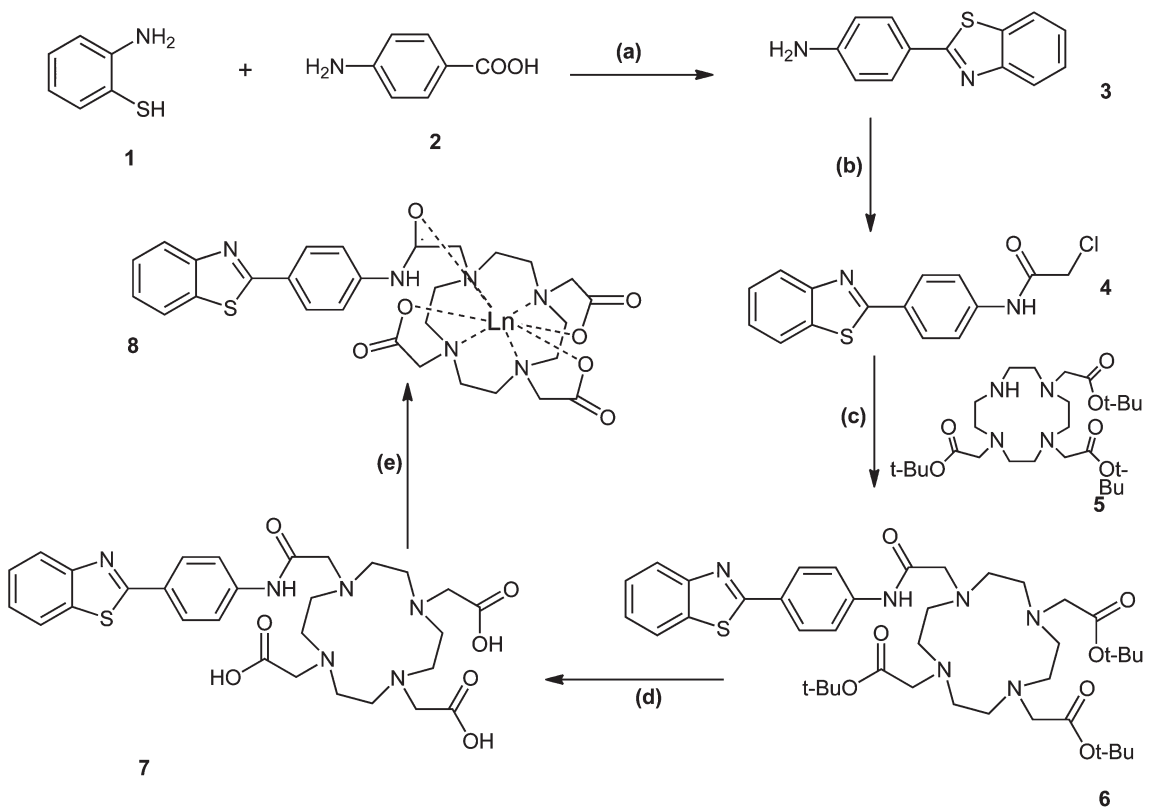

Scheme 1 Synthesis of Ln–DO3A-BT (Gd, Eu). Reagents and conditions: (a) polyphosphoric acid, 120 °C; (b) Cl–CH_2–CO–Cl, triethylamine (TEA), 0 °C–rt; (c) K_2CO_3, 70 °C, 12 h; (d) trifluoroacetic acid (TFA); (e) $LnCl_3$ (Ln = Gd, Eu), 70 °C, 14 h.

complexes were lyophilized and white solids were obtained in 90% and 93% yields, respectively. After the completion of both reactions, the reaction mixture was passed through chelex-100 at room temperature to trap the free Ln(III), and the absence of free Gd(III) was checked using a xylenol orange indicator.[29] Gd–DO3A-BT and Eu–DO3A-BT were characterized by mass spectrometry and the isotopic pattern of seven peaks and five peaks confirms the complexation of the ligand DO3A-BT with Gd and Eu, respectively.

Relaxometric studies

The presence of paramagnetic Gd(III) in the complexes resulted in an enhancement of the longitudinal relaxation rate of water protons ($1/T_1$). To express the proficiency of the Gd(III) complexes, relaxivity (r_1, $mM^{-1}\ s^{-1}$) values are used; relaxivity is the increase in the longitudinal proton relaxation rate and is measured using the Gd^{3+} complex at 1 mM concentration. Longitudinal and transverse ^1H spin relaxation rates have been measured for Gd–DO3A-BT in aqueous solution (pH = 7) at 6 different concentrations (0.625, 1.25, 2.5, 5, 10, and 20 mM). MR studies in the concentration range of 0.625–20 mM of Gd–DO3A-BT exhibited a contrast enhancement in T_1-weighted images with the effect being more pronounced at lower concentrations. Enhanced contrast was obtained at concentrations as low as 0.625 mM whereas a darker image intensity was obtained using higher concentrations of the complex. At low concentrations, an increase in the contrast results in an increase in signal intensity due to the effect on T_1 until the optimal concentration is reached. A further increase in concentration reduces the signal because of the effect on T_2. Longitudinal (T_1) and transverse (T_2) relaxation times of solvent-water protons as a function of DO3A-BT concentration (0.625–20 mM) were measured to investigate their relaxation behaviour.

The longitudinal relaxivity r_1, and transverse relaxivity r_2, was determined to be 4.18 $mM^{-1}\ s^{-1}$ and 4.54 $mM^{-1}\ s^{-1}$ respectively at 4.7 T and 37 °C. A plot of relaxivities as a function of the concentration of this complex is shown in Fig. 1 and a linear enhancement in the relaxivity with the concentration of the Gd complex is shown. The measured relaxivities arise from the exchange between the coordinated water molecules and the surrounding water molecules in solution. The DO3A-BT longitudinal relaxivity is approximately 35 times greater than that of LFB (r_1 = 0.09 $mM^{-1}\ s^{-1}$ at 4.7 T and 25 °C), which is an MR probe for differentiating myelinated regions.[27] It makes our compound superior to LFB as an MR contrast agent for imaging brain regions.

Inner sphere hydration number (q) determination

The number of water molecules directly coordinated to Gd^{3+} is one of the fundamental parameters influencing the relaxivity. To determine the hydration number, the luminescence lifetime decay of the $^5D_0$ excited state of the Eu(III) complex in H_2O and D_2O is measured. The luminescence lifetime studies established that OH oscillators of coordinated H_2O molecules

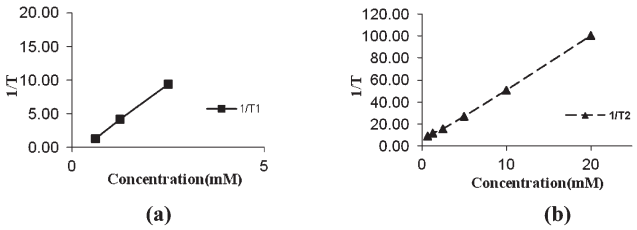

Fig. 1 (a) Longitudinal and (b) transverse relaxivity of Gd–DO3A-BTA.

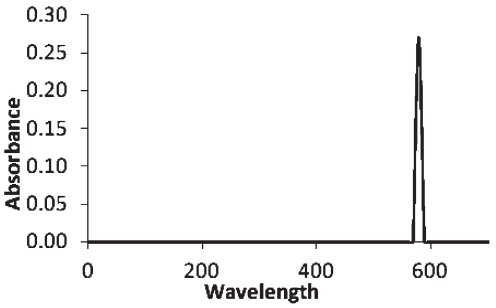

Fig. 2 Experimental UV-visible spectra of Eu(III)–DO3A-BT (25 °C, pH 7).

provide an efficient non-radiative pathway for the de-excitation of the emissive state of certain lanthanide ions. On the other hand, OD oscillators of coordinated D_2O molecules are quite inefficient in accomplishing this de-excitation. Thus, the different quenching frequencies of the O–H and O–D bonds give an estimation of the number of coordinated water molecules by using the equation developed by Supkowski and Horrocks.[30] The values for the luminescence lifetimes of Eu–DO3A-BT at pH 7.4 and 25 °C for the $^7F_0 \rightarrow {}^5D_0$ transition in H_2O and D_2O solutions are 638 μs and 2430 μs and the hydration number (q) is calculated to be 0.92, which clearly indicates a monoaqua Eu-coordinated system.

An interesting aspect of Eu(III) luminescence involves the $^7F_0 \rightarrow {}^5D_0$ excitation spectrum. Since the excited state and ground state are both nondegenerate and cannot be split further by the ligand field, each peak in the spectrum must correspond to a distinct Eu(III) environment. The absorption spectrum (Fig. 2) of Eu–DO3A-BT consists of a single peak due to the $^7F_0 \rightarrow {}^5D_0$ transition around 570 nm confirming the presence of a monoaqua complex.

Determination of the protonation and thermodynamic stability constants

We have summarized the protonation constant of DO3A-BT and the stability constant of the complex DO3A-BT with Gd^{3+}, Eu^{3+} and biologically active divalent metal cations obtained by potentiometric titration in Table 1 and 2 respectively.

A pH-potentiometric titration of the ligand DO3A-BT over the pH range 2–12 gave three protonation constants which are likely to be associated with the three carboxylic acid groups.

Table 1 Protonation constants (log K ± SD, n = 3) of the metal complexes DO3A-BT, DOTA and DTPA in NMe_4Cl (0.1 M) at 298 K with SD

	DOTA[31]	DTPA[31]	DO3A-BT
$\log K_1^H$	11.14 ± 0.02	10.49 ± 0.03	9.91 ± 0.06
$\log K_2^H$	9.69 ± 0.01	8.37 ± 0.05	8.22 ± 0.02
$\log K_3^H$	4.85 ± 0.07	4.09 ± 0.04	5.01 ± 0.05

Table 2 Stability constants (log β ± SD, n = 3) of the metal complexes DO3A-BTA, DOTA and DTPA (25 °C, μ = 0.1 M NMe_4Cl)

	DOTA[32]	DTPA[32]	DO3A-BT
$\log \beta_{GdL}$	23.2 ± 0.01	22.2 ± 0.04	18.4 ± 0.06
$\log \beta_{EuL}$	24.5 ± 0.06	20.0 ± 0.03	18.3 ± 0.02
$\log \beta_{Zn_2L}$	18.1 ± 0.06	16.5 ± 0.07	7.1 ± 0.04
$\log \beta_{Cu_2L}$	22.2 ± 0.03	22.4 ± 0.01	6.3 ± 0.04

The suitability of Gd^{3+} chelates for *in vivo* application is determined by their thermodynamic parameters. Most of the poly (aminocarboxylate) ligands form complexes with increasing stability across the lanthanide series. Here, the stability constant of DO3A-BT with Gd^{3+} falls almost in the same range as that of DOTA and DTPA but it is very low for Zn^{2+} and Cu^{2+}. These findings conclude that DO3A-BT forms exclusively stable complexes with Gd and does not undergo transmetallation with endogenous metal ions.

Kinetic stability

The aminopolycarboxylate complexes of Gd^{3+} are used as MR contrast agents and are kinetically inert compounds. However, a number of animal and human experiments indicate that the excretion of Gd^{3+} from the body is not complete, which is explained by assuming that a small amount of dissociation of Gd^{3+} from the Gd^{3+} complexes occurs *in vivo*. To understand the *in vivo* fate of the Gd^{3+} containing contrast agents, we have to know the rate of dissociation of the complex, which presumably takes place in the exchange reactions with endogenous metal ions. Thus sufficiently high thermodynamic stability of the Gd(III) complex and good selectivity of the chelating ligand for Gd(III) over other endogenous metal ions such as Cu^{2+} and Zn^{2+} are prerequisites for all biomedical applications. In order to obtain information on the rate of dissociation of the complex Gd–DO3A-BT, the kinetics of the exchange reactions were studied in 0.1 M KCl at 25 °C,

$$[\text{Gd–DO3A} - \text{BT}] + M^{n+} \rightleftharpoons [\text{M–DO3A} - \text{BT}] + Gd^{3+}$$

where M^{n+} = Zn^{2+} or Eu^{2+}. The rate of the exchange reactions were investigated in the presence of excess exchanging metal ions. The stability of Eu–DO3A-BT is similar to that of Gd–DO3A-BT and conversion occurs with 5–15 fold excess of Eu^{3+}. The log K_{ML} value (where K_{ML} is the stability constant of the metal–ligand complex) of the Zn(II) complex is lower than that of Ln–DO3A-BT (Ln = Eu, Gd) and despite the high stability of the Zn_2L complex, a large excess (50–80 fold) of metal ions is required for conversion. Pseudo first order rate constants of the metal exchange reactions of Gd–DO3A-BT along with other Gd complexes with Zn^{2+} and Eu^{2+} are shown in Table 3. Replacement of one carboxylate group with an amide group in Gd–DO3A-BT results in a slight decrease in the stability constant but has practically no effect on the kinetic stability of the Gd–DO3A-BT complex, which has a rate constant of 3.0×10^{-5} s^{-1}. This indicates that compared with the carboxylate group, the amide group has a lower reactivity with Zn^{2+} and thus it will not undergo transmetallation with endogenous metal ions.

Table 3 Pseudo first order rate constants characterizing the metal exchange reactions of Gd–DO3A-BT with Eu^{3+} and Zn^{2+} (25 °C, 0.1 M KCl)

	k_{obs} (s^{-1})	
Ligand	Eu^{3+}	Zn^{2+}
Gd–DO3A-BT		$3.0 \pm 0.7 \times 10^{-5}$
Gd–DOTA[33]	$2.1 \pm 0.2 \times 10^{-5}$	
Gd–DTPA[34]	$1.2 \pm 0.1 \times 10^{-3}$	$1.1 \pm 0.1 \times 10^{-5}$
Gd–DO3A[35]	$2.3 \pm 0.4 \times 10^{-3}$	$1.4 \pm 0.3 \times 10^{-2}$

^{99m}Tc radiocomplexation of DO3A-BT

The R_f of the labelled complex and free technetium was estimated using an instant thin layer chromatography method and was found to be 0.0 and 1.0, respectively, using acetone as a mobile phase. The optimum pH for radiolabelling was 6.0–7.5, and from the mole calculation, it was calculated that 52 μg of stannous chloride resulted in a maximum labelling efficiency with a minimum amount of $^{99m}TcO_4^-$. The labelling efficiency for ^{99m}Tc–DO3A-BT was calculated to be >98%, and was determined in a different solvent system chromatographically. The *in vitro* stability of ^{99m}Tc–DO3A-BT in the PBS buffer at pH 7.0 was checked at different time intervals: 4, 6, 24 and 48 h, and the percentage labelling efficiency at 48 h was found to be 95%, implying that the labelled conjugate was stable up to 48 h post labelling.

Blood kinetic study

The blood kinetics of ^{99m}Tc–DO3A-BT fits in to a two compartment model by regression analysis. The blood-activity curve studied in rabbits reveals a biphasic pattern of clearance with $t_{1/2}$ fast and $t_{1/2}$ slow. Initially the clearance of the agent exhibited a slow trend, but after 10 h the activity of ^{99m}Tc–DO3A-BT was greatly reduced. The biological half life was found to be $t_{1/2}(F)$ = 2 h and $t_{1/2}(S)$ = 13 h (Fig. 3). After 1 h, the ^{99m}Tc–DO3A-BT has approximately 20% activity remaining whereas only 3.1% remained after 24 h, which accounts for the excellent *in vivo* stability of the radioconjugate. This data correlates with the hydrophilic behaviour of the DO3A-like ligand as they are cleared from blood circulation mainly through the renal pathway.

Serum stability assay

In vivo kinetic inertness plays a critical role in determining competition experiments using native biological chelators

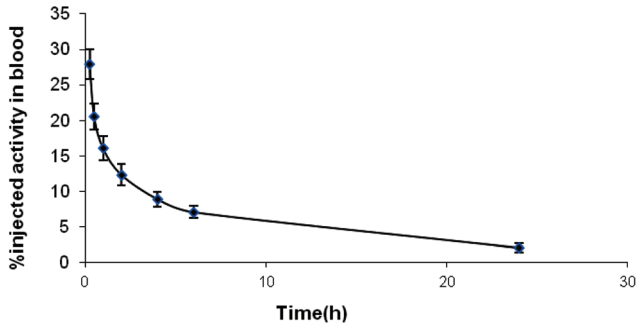

Fig. 3 Blood kinetics of ^{99m}Tc–DO3A-BT administered through the ear vein in a normal rabbit.

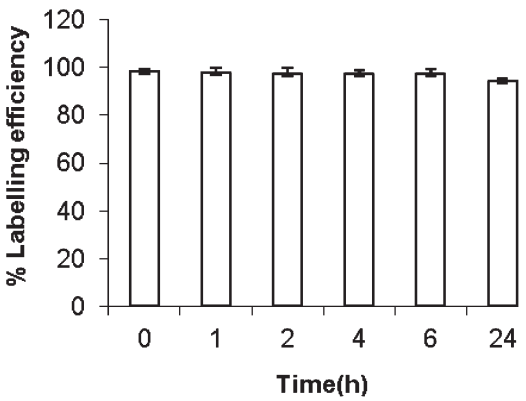

Fig. 4 *In vitro* serum stability of ^{99m}Tc–DO3A-BT at 37 °C (n = 3).

such as those contained in blood serum (*e.g.* apo-transferrin, albumin). *In vitro* assay is useful for predicting the *in vivo* stability and kinetic inertness of a radiometal ion complex. Lanthanides are trivalent metal ions, and behave similarly to Fe^{3+} cations that are present in blood such as transferrin, which is an iron transport protein in human serum. In addition to binding to iron, transferrin also forms complexes with lanthanides, and therefore the serum stability of these complexes is of major concern under physiological conditions.

^{99m}Tc–DO3A-BT demonstrated high serum stability as shown in Fig. 4 with approximately 95% of the radioactivity remaining after 24 h. The decomposition of ^{99m}Tc–DO3A-BT is slightly greater than DOTA and DTPA. The lower serum stability of the complex is due to a weaker octadentate structure for the DO3A-BT complex as compared to the octadentate structures of DTPA and DOTA. Lanthanide complexes generally require at least eight donor atoms to fully saturate their inner coordination sphere. DTPA and DOTA have eight potential atoms for metal coordination, whereas the eighth coordinating amide group of DO3A-BT is not as strong as the DTPA and DOTA carboxylate group, which explains the dissociation of the complex.

The human serum albumin (HSA) stability of the complex is further verified from a docking study of DO3A-BT with HSA having pdb id-1E78 which gave the following docking parameters:

Docking score	−6.655
Glide evdw	−30.946
Ecoul	−8.704
Glide energy	−39.651
Glide H-bond	−2.226

It is clear from the docking score that the DO3A-BT complex has considerably poor HSA binding affinity, which confirms the high serum stability of the complex. More negative docking scores indicate that the complex has a higher affinity for human serum albumin and a lower stability.

Binding affinity for neuronal cells

To determine the binding affinity of ^{99m}Tc–DO3A-BT to neuronal cells, a saturation binding assay was performed using increasing concentrations (10–0.001 mM) of the radioligand on brain homogenates. The percent specific binding of ^{99m}Tc–DO3A-BT was then measured as a function of the concentration of the radiolabeled complex. The data (Fig. 5) shows that when the concentration of ^{99m}Tc–DO3A-BT is increased there is an increase in the percentage uptake, which became saturated above 1 mM. The maximum percentage uptake for the brain homogenate was 78% with a 1 mM concentration of DO3A-BT. This study was performed to analyze the *in vitro* uptake of ^{99m}Tc–DO3A-BT which is further evaluated in *in vivo* biodistribution studies.

Biodistribution studies

The results of *in vivo* biodistribution studies in BALB/c mice showed that ^{99m}Tc–DO3A-BT is excreted through the renal pathway. It penetrates well through the intact blood–brain-barrier (BBB) when mannitol[36] is injected prior to injection of drug. The brain has a maximum uptake (1.2%) 15 min after the injection of the radiolabelled complex, but only 0.51% penetrates the brain when administered without mannitol as shown in Table 4 and 5. ^{99m}Tc–DO3A-BT displayed an initial brain penetration and a fast washout from the brain with only 0.06% ID g^{-1} remaining 1 h after injection. There was a significant correlation between log P and clearance as expressed by the 2 min to 30 min ratio. The least lipophilic compound cleared faster from the brain and the most lipophilic

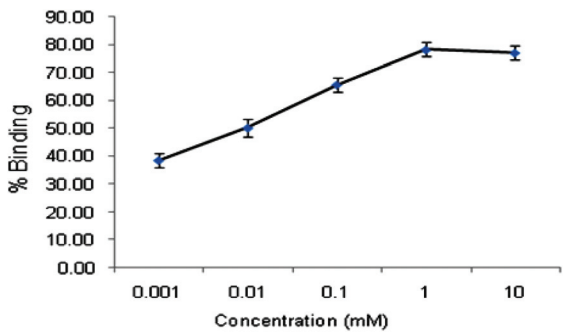

Fig. 5 The saturation binding assay of ^{99m}Tc–DO3A-BT in brain homogenate.

Table 4 The biodistribution profile of ^{99m}Tc–DO3A-BT in normal mice without mannitol (%ID g^{-1} ± SD, n = 3)

Organs	2 min	15 min	30 min	1 h
Blood	17.53 ± 0.93	12.42 ± 0.89	8.54 ± 0.71	2.60 ± 0.51
Brain	0.51 ± 0.03	0.12 ± 0.02	0.09 ± 0.01	0.02 ± 0.00
Heart	3.17 ± 0.71	6.81 ± 0.41	2.13 ± 0.29	0.94 ± 0.07
Liver	14.18 ± 2.30	12.13 ± 1.41	9.14 ± 0.93	7.15 ± 0.53
Spleen	9.15 ± 0.95	7.41 ± 0.54	5.61 ± 0.34	4.50 ± 0.24
Kidney	63.84 ± 1.14	15.11 ± 0.94	13.44 ± 0.73	5.50 ± 0.51
Stomach	0.87 ± 0.12	0.40 ± 0.17	0.20 ± 0.04	0.04 ± 0.01
Intestine	1.86 ± 0.51	0.89 ± 0.06	0.51 ± 0.04	0.04 ± 0.00

Table 5 The biodistribution profile of ^{99m}Tc–DO3A-BT in normal mice with mannitol (%ID g^{-1} ± SD, n = 3)

Organs	2 min	15 min	30 min	1 h
Blood	19.87 ± 0.91	15.13 ± 1.01	9.84 ± 1.51	2.46 ± 0.99
Brain	0.87 ± 0.17	1.20 ± 0.51	0.54 ± 0.07	0.06 ± 0.01
Heart	8.60 ± 1.23	9.45 ± 1.09	3.76 ± 0.91	0.68 ± 0.08
Liver	13.19 ± 1.14	10.31 ± 1.31	11.71 ± 1.02	8.10 ± 0.06
Spleen	5.06 ± 1.13	2.89 ± 0.90	2.33 ± 0.13	1.37 ± 0.09
Kidney	43.59 ± 2.10	19.39 ± 2.91	15.26 ± 2.63	7.53 ± 1.92
Stomach	0.73 ± 0.05	0.35 ± 0.02	0.87 ± 0.06	0.61 ± 0.08
Intestine	2.50 ± 0.41	2.33 ± 0.23	1.91 ± 0.45	0.59 ± 0.08

compound accumulated in the brain over 30 min. The log P value of DO3A-BT–Gd is 2.27 whereas for ^{99m}Tc–DO3A-BT log P = −1.189, which indicates that there is no need to inject mannitol when using DO3A-BT–Gd, but due to the hydrophilic nature of ^{99m}Tc–DO3A-BT, mannitol is required for the disruption of the BBB.

Experimental

Materials

All reagents and solvents were used in the purest grade that was available commercially without further purification. 1,4,7,10-Tetraazacyclododecane was purchased from Strem, France. 2-Aminothiophenol, *tert*-butylbromoacetate, 4-aminobenzoic acid, polyphosphoric acid, anhydrous gadolinium trichloride, 2-chloroacetylchloride, potassium carbonate, acetonitrile, methanol, trifluoroacetic acid, HPLC water, dichloromethane, chloroform and triethylamine were purchased from Aldrich, Germany. Column chromatography was carried out using silica MN60 (60–200 μm), TLC on aluminium plates coated with silica gel 1160, F_{254} (Merck).

Instrumentation

^{1}H and ^{13}C NMR spectra were recorded using a Bruker Avance II 400 MHz. Chemical shifts are reported relative to TMS. ESI-MS was performed using the Agilent 6310 system, Germany, with the ion trap detection in the positive and negative mode.

Synthesis of 4-benzothiazol-2-yl-phenylamine (3). 2-Aminobenzenethiol (2.34 ml, 0.02 mmol) was added to the solution of 4-aminobenzoic acid (3 g, 0.02 mmol) in polyphosphoric acid (30 ml). The reaction mixture was heated to 130 °C for 5 h. The reaction mixture was cooled to room temperature and neutralized with 10% Na_2CO_3 (300 ml). A yellow solid precipitated from the reaction mixture and was filtered under reduced pressure to give the desired product (**3**). Yield (5.50 g, 91.6%). R_f: 0.8 (9 : 1; DCM–MeOH). Elemental analysis: found C, 68.01; H, 4.21; N, 12.99; S, 14.35. Calc. for ($C_{13}H_{10}N_2S$): C, 69.00; H, 4.45; N, 12.38; S, 14.17. ^{1}H NMR (400 MHz, DMSO-d_6, Me_4Si): δ_H = 6.75 (d, 2H, J = 8.7 Hz, CH), 7.32 (t, 1H, CH), 7.44 (t, 1H, CH), 7.78 (d, 2H, J = 8.4 Hz, CH), 7.89 (d, 1H, J = 8.0 Hz, CH), 7.97 (d, 1H, J = 7.6 Hz, CH). ^{13}C NMR (100 MHz, DMSO-d_6, Me_4Si): δ_C = 154.21, 151.42, 134.18, 129.22, 126.72, 124.88, 122.39, 122.26, 114.80, 68.46 (C═N). ESI-MS: m/z found 227 $[M + H]^+$ ($C_{13}H_{10}N_2S$), calculated 226.

Synthesis of *N*-(4-benzothiazol-2-yl-phenyl)-2-chloroacetamide (4). To a stirred solution of **3** (1 g, 4.42 mmol) in dried CH_2Cl_2 (20 ml), Et_3N (0.92 ml, 6.64 mmol) and chloroacetylchloride (0.42 ml, 5.30 mmol) in CH_2Cl_2 (5 ml) were added drop wise to the reaction mixture at 0 °C. The reaction mixture was stirred for 1 h at 0 °C and then was stirred further for 24 h at room temperature. The completion of the reaction was monitored by TLC and on completion, the reaction mixture was filtered and evaporated under reduced pressure to give the crude product. The trituration of the crude product gave a pure white powder. Yield (1.43 g, 80%). R_f: 0.66 (8 : 2; DCM–MeOH). Elemental analysis: found C, 59.22; H, 3.99; N, 8.99; S, 11.06. Calc. for ($C_{15}H_{11}ClN_2OS$): C, 59.50; H, 3.66; N, 9.25; S, 10.59. ^{1}H NMR (400 MHz, DMSO-d_6, Me_4Si): δ_H = 4.34 (s, 2H, CH_2), 7.44 (t, 1H, CH), 7.53 (t, 1H, CH), 7.82 (d, 2H, J = 8.8 Hz, CH), 8.02 (d, 2H, J = 6.4 Hz, CH), 8.1 (d, 2H, J = 7.6 Hz, CH). ^{13}C NMR (100 MHz, DMSO-d_6, Me_4Si): δ_C = 167.33 (C═N), 165.59 (C═O), 154.01, 141.87, 134.74, 128.53, 127.06, 125.77, 123.05, 122.75, 120.00, 44.03. ESI-MS: m/z found 338 $[M + K - 2H]^-$ ($C_{15}H_{11}ClN_2OS$), calculated 302.

Synthesis of 1,4,7-tri(*tert*-butoxymethane)-1,4,7,10-tetraazacyclododecane (*t*-Bu-DO3A) (5). $NaHCO_3$ (1.3 g, 15.5 mmol) was added to a solution of 1,4,7,10-tetraazacyclododecane (1 g, 5.18 mmol) in dry acetonitrile (30 ml) at 0 °C under a nitrogen atmosphere and stirred for 0.5 h. *tert*-Butylbromoacetate (2.29 ml, 15.5 mmol) in acetonitrile (5 ml) was added slowly to the above reaction mixture at 0 °C and stirred for 40 h at room temperature. The progress of the reaction was monitored by TLC (9 : 1; DCM–methanol). After the completion of the reaction, the reaction mixture was filtered and the filtrate was evaporated to dryness. The crude compound was purified by column chromatography (silica gel, 10% methanol in dichloromethane) to give a white powder of *t*-Bu-DO3A (2.30 g, 80%). R_f: 0.65 (9 : 1; DCM–MeOH). Elemental analysis: found C, 60.33; H, 9.05; N, 10.56. Calc. for ($C_{26}H_{50}N_4O_6$): C, 60.67; H, 9.79; N, 10.89. ^{1}H NMR (400 MHz, $CDCl_3$, Me_4Si): δ_H = 1.45 (s, 27H, $C(CH_3)_3$), 2.85 (d, J = 10 Hz, 12H, 6 × CH_2), 3.03 (s, 4H, 2 × CH_2), 3.36 (s, 6H, 3 × CH_2). ^{13}C NMR (100 MHz, $CDCl_3$, Me_4Si): δ_C = 170.54, 169.65 (C═O), 81.86 ($C(CH_3)_3$), 47.48, 48.81, 49.17, 51.30 (CH_2), 28.21 (CH_3). ESI-MS: m/z found 515 $[M + H]^+$ ($C_{26}H_{50}N_4O_6$), calculated 514.

Synthesis of 10-[*N*-(4-benzothiazol-2-yl-phenylcarbamoyl)-methyl]-1,4,7-tri(carbobutoxy-methane)-1,4,7,10-tetraaza-cyclododecane (6). 1,4,7-Tris(carbobutoxymethane)-1,4,7,10-tetraazacyclododecane (1 g, 1.94 mmol) was dissolved in dry acetonitrile (20 ml). K_2CO_3 (2.15 g, 15.5 mmol) was added to the reaction mixture and stirred at room temperature for 0.5 h. *N*-4-Benzothiazol-2-yl-phenyl-2-chloroacetamide (0.58 g, 1.94 mmol) was added to the reaction mixture and heated to 70 °C. After 14 h the reaction mixture was filtered and evaporated under reduced pressure to give a crude oily residue. The compound was purified by column chromatography to give a yellow oil (yield 0.83 g, 60%). R_f: 0.34 (8 : 2; DCM–MeOH). Elemental analysis: found C, 62.97; H, 7.65; N, 10.98; S, 4.24. Calc. for ($C_{41}H_{60}N_6O_7S$): C, 63.05; H, 7.74; N, 10.76; S, 4.11. ^{1}H NMR (400 MHz, MeOD, Me_4Si): δ_H = 1.52 (s, 9H, $C(CH_3)_3$), 2.09 (b, 8H, CH_2), 2.79 (b, 4H, CH_2), 3.24 (s, 6H, CH_2), 3.14 (s, 4H, CH_2), 3.31 (s, 2H, CH_2), 8.08 (d, J = 8.2 Hz, 3H), 7.84 (d, J = 7.8 Hz, 1H), 7.54 (t, 1H), 7.45 (t, 1H). ^{13}C NMR (100 MHz, MeOD, Me_4Si): δ_C = 173.12, 171.54, 168.14, 153.63, 141.70, 134.44, 128.19, 127.57, 126.34, 125.15, 122.08, 121.57, 119.62, 56.32, 55.35, 55.26, 26.99. ESI-MS: m/z found 782 $[M + 2H]^+$ and 804 $[M + Na]^+$ ($C_{41}H_{60}N_6O_7S$), calculated 780.

Synthesis of {4-[(4-benzothiazol-2-yl-phenylcarbamoyl)-methyl]-7,10-bis-carboxymethyl-1,4,7,10-tetraazacyclododec-1-yl}-acetic acid (DO3A-BT) (7). Compound **6** (400 mg, 0.51 mmol) was dissolved in 5 ml of neat trifluoroacetic acid at 0 °C and stirred for 5 h. The solvent was evaporated under reduced pressure. After trituration with cold ether, the compound precipitated as a white powder The compound was dried, dissolved in water and neutralized to pH 7 by the addition of 1 M NaOH. The product was obtained as brown solid. Yield (283 mg, 75%). Elemental analysis: found C, 57.09; H, 6.11; N, 13.35; S, 5.55. Calc. for ($C_{30}H_{37}N_5O_7S$): C, 56.85; H, 5.92; N, 13.72; S, 5.23. ^{1}H NMR (400 MHz, D_2O, Me_4Si): δ_H = 2.59–3.85 (m, 26H, CH_2), 7.02 (s, 1H, CH), 7.16–7.26 (m, 6H, CH), 7.56 (s, 1H, CH). ^{13}C NMR (100 MHz, D_2O, Me_4Si): δ_C = 38.69, 42.24, 47.72, 49.00, 50.08, 51.68, 53.09, 54.83, 117.43, 119.69, 127.09, 163.07, 174.37, 178.61. ESI-MS: m/z found 614 $[M + H]^+$ ($C_{30}H_{37}N_5O_7S$), calculated 613.

Synthesis of lanthanide(III) complexes with DO3A-BT (Ln–DO3A-BTA) (8). The pH of the ligand DO3A-BTA (500 mg, 0.81 mmol) was adjusted to 7.0 by the drop wise addition of 1 M NaOH. Anhydrous $LnCl_3$ ($GdCl_3$ and $EuCl_3$) (257 mg, 0.98 mmol) was added to the above reaction mixture and stirred for 18 h at 70 °C and pH kept at 7.0. After 18 h, the reaction mixture was cooled and passed through chelex-100 at room temperature to trap the free lanthanide. The absence of free Gd(III) was checked by using xylenol orange as an indicator. The crude product was filtered, evaporated and lyophilized to get the desired product as a white solid. Elemental analysis: found C, 43.09; H, 4.02; N, 9.99; S, 4.76. Calc. for ($C_{29}H_{33}GdN_6O_7S$): C, 45.42; H, 4.34; N, 10.96; S, 4.18. ESI-MS: m/z (Gd–DO3A-BT) found 768 $[M]^+$, 790 $[M + Na]^+$, calculated 768. Elemental analysis: found C, 46.22; H, 5.12; N, 12.04; S, 4.56. Calc. for ($C_{29}H_{33}EuN_6O_7S$): C, 45.73; H, 4.37; N, 11.03; S, 4.21. ESI-MS: m/z (Eu–DO3A-BT) found 763 $[M]^+$, 785 $[M + Na]^+$, calculated 763.

In vitro relaxivity measurement

Experiments were carried out using a 4.7 Tesla horizontal Bruker Biospect 47/50 (Bruker, Ettlingen, Germany). The system was equipped with a 12 cm BG12 gradient system capable of 193 mT m^{-1}. Measurements were performed with a birdcage resonator (60 mm in diameter and 120 mm long) tuned to 20 MHz. T_1 measurements were performed at 37 °C using an Inversion-Recovery scheme (increment of inversion delay: 10 ms with 456 increments) followed by a RARE imaging sequence (TR/TEeff: 5000/2.6 ms; FOV (field of view): 30 × 30 mm; matrix: 128 × 128; slice thickness: 1 mm). T_2 measurements were performed with a Carr–Purcell–Meiboon–Gill imaging sequence (TR: 2500 ms; inter-echo time: 11.6 ms; number of echoes: 64; FOV: 30 × 30 mm; matrix: 128 × 128; slice thickness: 1 mm). Relaxation data were analyzed with home-made software developed on Igor Pro (Wave metrics, Lake Oswego, OR, USA).

To measure the changes in the longitudinal relaxivity (r_1), MRI experiments were performed at six different concentrations (0.625–20 mM) of [GdL] prepared in phosphate buffered saline in 1.5 mL Eppendorf tubes at physiological pH. Each tube was filled with 400 μL of the contrast agent solution. Relaxivity at different concentration was then calculated using eqn (1):

$$r_{1,obs} = (1/T_{1,obs} - 1/T_{1,d})/[GdL] \quad (1)$$

where $T_{1,obs}$ is the measured T_1; $T_{1,d}$ is the diamagnetic contribution of the solvent and [GdL] is the concentration in mmol of the appropriate Gd(III) complex.

Equilibrium measurements

Potentiometric titrations for the determination of the ligand protonation constant and stability constant of the complexes with Gd(III), Eu(III), Cu(II) and Zn(II) were measured with an automatic titration system consisting of a Metrohm 713 pH meter equipped with a Metrohm A.60262.100 glass electrode, 800 Dosino autoburet. It has a precision of ±0.002 pH unit and is thermostated (25 °C) with a glass-jacketed titration cell fitted with a combination glass electrode and a Metrohm piston buret with a capillary tip placed below the surface of the sample. This avoids absorption of CO_2 by the base solution. The pH meter–electrode system was calibrated with standard buffers. The protonation constants of DO3A-BT were determined potentiometrically by titrating 1 mM of DO3A-BT with 10 mM tetramethylammoniumhydroxide (TMAOH). Potentiometric titrations were carried out with 0.1 M ionic strength of tetramethylammoniumchloride (TMACl) at 25 °C. Titrations were performed in the pH range of 2–12 for protonation constants.

The stability constants of DO3A-BT with Gd(III), Eu(III), Cu(II) and Zn(II) were determined by direct pH potentiometric titration (0.002–0.004 M M^{n+} and 0.002 M ligand solutions),

I = 0.1 M using TMACl. Solutions of Gd(III), Eu(III) and Cu(II) were prepared by dissolving the appropriate amounts of their salts in milliQ water. For titrations of the complexes, an appropriate volume of the previously prepared metal solution was added *via* a micropipette to reach the 1 : 1 ligand to metal ratio. A minimum of two duplicate measurements were taken. The protonation and stability constants were evaluated using titration data using the program *Tiamo* 2.0. The protonation constant of ligand is expressed by eqn (2) and the stability constant of the metal complex is given by eqn (3):

$$K_i = \frac{[H_iL]}{[H_{i-1}L][H^+]} \quad (2)$$

$$K_{MH_iL} = \frac{[MH_iL]}{[MH_{i-1}L][H^+]} \quad i = 0,\ 1,\ 2,\ 3 \quad (3)$$

Kinetic measurement

High kinetic stability is an important requirement for Gd^{3+} complexes that are used as contrast enhancement agents in MRI. The extent of the dissociation depends on the selectivity of the ligand for Gd^{3+} over the endogenous metal ions present in body fluids. For example, *in vivo*, endogenous cations (Fe^{3+}, Ca^{2+}, Zn^{2+} and Cu^{2+}) can react with Gd chelates by displacing Gd^{3+} in a metal–metal transmetallation exchange. Thus to understand the *in vivo* fate of the Gd^{3+} containing contrast agent, we have to know the rate of the exchange reaction of Gd–DO3A-BT with Eu^{3+} and Zn^{2+}. The rate of the metal exchange reactions of Gd–DO3A-BT with Eu^{3+} and Zn^{2+} were studied using a UV-visible spectrophotometer, following the formation of the Eu^{3+} and Zn^{2+} complexes at 280 and 317 nm, respectively. The concentration of the complex Gd–DO3A-BT was 6.2×10^{-5} M, whereas the concentration of the metal ion was 30–40 times higher, respectively, guaranteeing pseudo-first-order conditions. The temperature was maintained at 25 °C and the ionic strength of the system was kept constant with 0.1 M KCl at pH 7.4. In the presence of an excess of the exchanging ion, the transmetallation process may be assumed to be a pseudo-first-order process and the rate of reaction can be expressed with eqn (4),

$$A_t = (A_o - A_p)e^{-k_{obs}t} \quad (4)$$

where k_{obs} is a pseudo-first-order rate constant and A_t, A_o, and A_p are the absorbance values at time t, and at the starting and equilibrium points of the reaction, respectively.

UV-visible absorption and luminescence measurement

The inner sphere hydration number of Eu–DO3A-BT was recorded on a Cary Varian double beam UV/visible spectrophotometer with Perkin-Elmer Luminescence Cells with a path length of 1 cm at 293 K. The luminescence lifetime τ_L was calculated by measuring the decay at the maximum of emission spectra and the signals were analysed as single exponential decays. The instrument settings were: gate time = 10 ms, integration time = 1 s, flash count = 8 and proper slit widths were used for no saturation of the signal by using a different delay times. Solutions of the Eu–DO3A-BT complex were prepared *in situ* by mixing its appropriate volume in milliQ water or in D_2O with the ligand in Tris buffer 0.1 M (pH = 7.4) or in D_2O followed by the addition of NaOD until pH = 7. The excitation source was a hydrogen gas filled nanosecond flash lamp with a low hydrogen gas pressure of 0.4 bar operating at a frequency of 40 kHz. The slit widths for both the excitation and emission monochromators are kept open. The intensity decay curves were obtained at emission maximum and fitted as sum of exponentials as:

$$I_t = I_0 \sum A_i \exp(-t/\tau_i) \quad (5)$$

where, τ_i and A_i represent the fluorescence lifetime and pre exponential factor for ith component. The number of coordinated water molecules (q) present in the inner sphere of the complex is calculated from the luminescence rate constants of Eu–DO3A-BT in light and heavy water using equation developed by Supkowski and Horrocks for Eu(III):[30]

$$q = A_{Eu}(1/\tau_{H_2O} - 1/\tau_{D_2O} - a_{Eu}) \quad (6)$$

where τ_{H_2O} and τ_{D_2O} are the luminescence lifetimes in H_2O and D_2O,[37] giving an inner sphere hydration number. The value of A_{Eu} = 1.11 ms and a_{Eu} = 0.31 ms^{-1}; a_{Eu} is used for the correction of error which accounts for closely diffusing OH oscillators.

Biological studies

^{99m}Tc radiocomplexation of DO3A-BT

DO3A-BT (2 μmol) was dissolved in 1 ml of doubly distilled water. 100 μl of this solution was taken in a shielded glass vial and stannous chloride (1 μmol, dissolved in 1 ml of 10% acetic acid purged with N_2) was added to it, followed by the addition of 100 μl of 74 MBq of freshly eluted (<1 h) ^{99m}technecium pertechnetate saline solution. The pH of the reaction mixture was adjusted to 7 using 0.1 M sodium carbonate solution. All contents were thoroughly mixed and incubated for 30 min at room temperature to achieve an optimal labelling yield.

Radiochemical purity of ^{99m}Tc–DO3A-BT complex

The radiolabelling efficiency of the above complex was determined by using ascending instant thin layer chromatography ITLC-SG (Paul Gelman, USA) using 100% acetone simultaneously with pyridine–acetic acid–water (PAW) (3 : 5 : 1.5) and saline. TLC strips were cut into 0.5 cm fragments and counts of each fragment were taken. The percentage of free Na $^{99m}TcO_4^-$, reduced ^{99m}Tc and complexed ^{99m}Tc could be calculated from this method. Complexed ^{99m}Tc remained at the origin whereas uncomplexed ^{99m}Tc moved with the solvent front.

Blood kinetics

Blood clearance studies were carried out using normal rabbits and 0.1 ml of ^{99m}Tc–DO3A-BT was administered intravenously through the dorsal ear vein of the animal. Blood samples (10 μl) were collected at different time intervals and the radioactivity was counted using a NaI well type gamma counter. The percentage radioactivity in the whole blood was calculated assuming that the whole blood volume is 7% of the body weight.

Human serum stability

Human serum was prepared by allowing blood collected from healthy volunteers to clot for 1 h at 37 °C in a humidified incubator maintained at 5% carbon dioxide/95% air. Then, the samples were centrifuged at 400 *g*, and the serum was filtered through a 0.22 μm syringe filter into sterile plastic culture tubes. The radio labelled DO3A-BT was immediately placed in a CO_2 chamber, incubated at 37 °C and then analyzed to check for any dissociation of the complex. The percentage of free pertechnetate at a particular time point was estimated using acetone and pyridine, acetic acid, and water (PAW) (3 : 5 : 1.5) as the mobile phase which represent the percentage dissociation of the complex at that particular time point in serum. The HSA binding of the complex is also determined from docking experiments carried out by using GLIDE (grid based ligand docking with energetic) and a ligand docking programme in extra precision (XP) mode using HSA pdb id-1E78.

Radioligand binding assay for neuronal cells

BALB/c mice were sacrificed, and their brains were excised and homogenized in 0.1 M phosphate buffer (pH = 8). An 0.4 ml aliquot of the brain homogenate was added to Eppendorf tubes containing different concentrations of ^{99m}Tc–DO3A-BT (10–0.001 mM) and incubated for 30 min at 37 °C. After incubation, 0.1 ml of 10% trichloroacetic acid was added to each Eppendorf tube which caused the protein to precipitate out. Then samples were centrifuged and washed twice with PBS to obtain a pellet of protein which was then resuspended in PBS. The uptake of ^{99m}Tc radioactivity in each sample was measured with an automated gamma scintillation counter and was normalized with ^{99m}Tc-decay correction as well as for diluted homogenates. Percentage uptake in the brain was plotted against the different concentrations of ^{99m}Tc–DO3A-BT used in the binding assay.

Biodistribution in BALB/c mice

Animal models

All animal experiments were done in accordance with the guidelines of the Indian Animal Ethics Committee. BALB/c mice were used for blood clearance and biodistribution. Mice were housed on a normal diet of sterile food pellets and water at a controlled temperature of 22 ± 2 °C.

A biodistribution study of ^{99m}Tc–DO3A-BT was performed on BALB/c mice (25–30 g) with and without mannitol, as mannitol disrupts the BBB due to osmotic shock. MR contrast agents (Gd chelates) in combination with mannitol allow the contrast agent to cross the BBB. 30% of mannitol was injected 5 min before the injection of the drug. An aliquot of 2 mCi of ^{99m}Tc–DO3A-BT was injected in each mouse intravenously through the tail vein and the animals were humanely sacrificed at 5, 15, 30, 60 min post injection. Tissue samples including the lung, liver, spleen, kidney, stomach, blood, heart, intestine and brain were removed and weighed. Uptake of ^{99m}Tc radioactivity in each sample was measured as %ID g^{-1} of the tissue with an automated gamma scintillation counter and was normalized using the ^{99m}Tc-decay correction.

Summary

We have designed a biocompatible probe which can investigate the brain non-invasively, and represents a platform for the development of multimodal imaging tools for neuroscience. We have presented the synthesis and characterization of a dual modality imaging agent Ln–DO3A-BT (Ln = Gd or Eu), which was proved to be an excellent MR contrast and optical imaging agent. Its longitudinal relaxivity is ~35 times higher than that of LFB which is a selective MR contrast agent for the brain commonly found in the literature. The described macrocyclic complex fulfils the requirements of a luminescent probe as an optical agent: it has a good hydrophilicity and a high kinetic inertness in aqueous solutions. Moreover the pharmacokinetic profile of ^{99m}Tc–DO3A-BT showed a good serum stability, a fast clearance through the renal route and a substantial brain uptake when injected along with 30% mannitol. The highest *in vitro* binding affinity for neuronal cells makes it highly specific for mapping brain regions.

Acknowledgements

We are highly thankful to Dr R. P. Tripathi, Director INMAS, for providing the necessary facilities. This work was supported by the Council of Scientific and Industrial research (CSIR) and the Defence Research and Development Organization, Ministry of Defence, under R&D project INM-311(3.1).

References

1 M. Filippi, A. Falini, D. L. Arnold, F. Fazekas, O. Gonen, H. J. Simon, V. Dousset, M. Savoiardo and J. S. Wolinsky, *J. Magn. Reson. Imaging*, 2005, **21**, 669–675.
2 A. Mishra, A. Schuz, J. Engelmann, M. Beyerlein, N. K. Logothetis and S. Canals, *ACS Chem. Neurosci.*, 2011, **2**, 578–587.
3 V. Comblin, D. Gilsoul, M. Hermann, V. Humblet, V. Jacques, M. Mesbahi, C. Sauvage and J. F. Desreux, *Coord. Chem. Rev.*, 1999, **186**, 451–470.

4 M. Botta, *Eur. J. Inorg. Chem.*, 2000, **3**, 399–407.
5 S. Aime, C. Cabella, S. Colombatto, S. G. Crich, E. Gianolio and F. Maggioni, *J. Magn. Reson. Imaging*, 2002, **16**, 394–406.
6 K. M. Hasebroock and N. J. Serkova, *Expert Opin. Drug Metab. Toxicol.*, 2009, **5**, 403–416.
7 M. Li and P. R. Selvin, *J. Am. Chem. Soc.*, 1995, **117**, 8132–8138.
8 F. S. Richardson, *Chem. Rev.*, 1982, **82**, 541–552.
9 M. T. Vlaardingerbroek and J. A. Boerden, *Magnetic Resonance Imaging. Theory and Practice*, Springer Verlag, Germany, 1996, 242–243.
10 P. Caravan, *Chem. Soc. Rev.*, 2006, **35**, 512–523.
11 A. Bianchi, L. Calabi, F. Corana, S. Fontana, P. Losi, A. Maiocchi, L. Paleari and B. Valtancoli, *Coord. Chem. Rev.*, 2000, **204**, 309–393.
12 P. Herman, J. Kotek, V. Kubicek and I. Lukes, *Dalton Trans.*, 2008, 3027–3047.
13 K. W.-Y. Chan and W.-T. Wong, *Coord. Chem. Rev.*, 2007, **251**, 2428–2451.
14 E. Brucher, *Top. Curr. Chem.*, 2002, **221**, 103–122.
15 P. Caravan, J. J. Ellison, T. J. McMurry and R. B. Lauffer, *Chem. Rev.*, 1999, **99**, 2293–2352.
16 S. Aime, M. Botta, M. Fasano, S. G. Crich and E. Terreno, *Coord. Chem. Rev.*, 1998, **27**, 19–29.
17 A. Bianchi, L. Calabi, C. Giorgi, P. Losi, P. Mariani, P. Paoli, P. Rossi, B. Valtancoli and M. Virtuani, *J. Chem. Soc., Dalton Trans.*, 2000, **5**, 697–705.
18 E. Toth, L. Helm and A. E. Merbach, *Top. Curr. Chem.*, 2002, **221**, 61–101.
19 K. N. Raymond and V. C. Pierre, *Bioconjugate Chem.*, 2005, **16**, 3–8.
20 M. F. Loncin, J. F. Desreuk and E. Merciny, *Inorg. Chem.*, 1986, **25**, 2646–2648.
21 X. Wang, T. Jin, V. Comblin, L. M. Antonio and E. Merciny, *Inorg. Chem.*, 1992, **31**, 1095–1099.
22 G. R. Choppin and Z. M. Wang, *Inorg. Chem.*, 1997, **36**, 249–252.
23 W. D. Horrocks and D. R. Sudnick, *J. Am. Chem. Soc.*, 1979, **101**, 334–340.
24 M. Albin and W. D. Horrocks, *Inorg. Chem.*, 1985, **24**, 895–900.
25 D. Alagille, R. M. Baldwin and G. D. Tamaganan, *Tetrahedron Lett.*, 2005, **46**, 1349–1351.
26 G. Henriksen, A. I. Hauser, A. D. Westwell, B. H. Yousefi, M. Schwaiger, A. Drzezga and H. J. Wester, *J. Med. Chem.*, 2007, **50**, 1087–1089.
27 M. L. Blackwell, C. T. Farrar, B. Fischl and B. R. Rosen, *NeuroImage*, 2009, **46**, 382–393.
28 C. A. Mathis, W. E. Klunk, Y. Wang, D. P. Holt, G. F. Huang and M. L. Debnath, *J. Med. Chem.*, 2003, **46**, 2740–2754.
29 A. Barge, G. Cravoyyo, E. Gianolio and F. Fedeli, *Contrast Media Mol. Imaging*, 2006, **1**, 184–188.
30 R. M. Supkowski and W. D. Horrocks, *Inorg. Chim. Acta*, 2002, **340**, 44–48.
31 G. Anderegg, F. Arnaud-Neu, R. Delgado, J. Felcman and J. K. Popov, *Pure Appl. Chem.*, 2005, **77**, 1445–1495.
32 M. Port, J. M. Idée, C. Medina, C. Robic, M. Sabatou and C. Corot, *BioMetals*, 2008, **21**, 469–490.
33 E. Toth, E. Bucher, I. Lazar and I. Toth, *Inorg. Chem.*, 1994, **33**, 4070–4076.
34 Z. Jaszberenyi, I. Bonyai, E. Bucher, R. Kiraly, K. Hideg and T. Kalai, *Dalton Trans.*, 2006, 1082–1091.
35 K. Kumar, C. A. Chang and M. F. Tweedle, *Inorg. Chem.*, 1993, **32**, 587–593.
36 Y. Z. Wadghiri, E. M. Sigurdsson, J. I. Elliott, H. Scholtzova, C. Y. Tang, G. Aguinaldo, M. Pappolla, K. Duff, T. Wisniewski and D. H. Turnbull, *Magn. Reson. Med.*, 2003, **50**, 293–302.
37 A. Beeby, I. M. Clarkson, R. S. Dickins, S. Faulkner, D. Parker, A. S. Desouza, J. A. G. Williams and M. Woods, *J. Chem. Soc., Perkin Trans. 2*, 1999, 493–503.